Conf-911003--21

DYNAMIC MATERIAL PROPERTIES OF REFRACTORY MATERIALS:

MOLYBDENUM

SAND--91-0679C

DE92 003577

M. D. Furnish and L. C. Chhabildas

Sandia National Laboratories, Albuquerque, N. M. 87111

Abstract

Recently, techniques have been developed to determine dynamic material properties of refractory metals at strain rates of 10^5 to 10^{10} sec^{-1} and to stresses approaching 250 GPa. Similar techniques have been used to measure the dynamic properties of molybdenum; results are summarized in this paper. These experiments have allowed the determination of pressure and loading rate effects on the dynamic yield strength of molybdenum and its viscoelastic properties, as well as a determination of the Hugoniot, at relatively low stresses. Several combinations of loading and reloading and loading and unloading cycles have been employed, utilizing a compressed gas gun and VISAR diagnostics. Pressure ranges from 6.5 to 15 GPa were investigated with specimen thicknesses ranging from 1.5 to 13 mm. The Hugoniot is consistent with earlier observations at higher pressures. The Hugoniot elastic limit appears to decrease slightly with distance over the stress range reported in this study, although the decrease is of the same order as the uncertainties. Otherwise, waves are observed to be steady. Strengths at the HEL and the Hugoniot state, approximately 1.5 GPa, are within the range observed for lower strain rates of 10^{-3} sec^{-1} to $5 \cdot 10^3$ sec^{-1}, consistent with a thermal activation slip model applicable across a wide range of strain rates. Strain rate behaves as approximately as the fourth power of stress, although it appears to decrease with propagation distance over the specimen thickness range used.

Introduction

With the evolution of time-resolved interferometry techniques[1,2] for measuring shock wave structures, it has become possible to conduct experiments yielding far more information than previously possible for constraining material models[3,4]. In addition to Hugoniot data, information can be obtained about yield strengths, shock viscosity, release trajectories, multiwave structures and the strength of materials in the shocked state. Techniques have been developed to determine the dynamic material properties at strain rates of 10^5 to 10^{10} sec^{-1} at stresses approaching 250 GPa[5,6,7,8]. In particular, rate-dependant effects and release hystereses can be characterized. These sets of data are crucial in evaluating strain-rate-dependant viscoelastic material models.

As part of an effort to characterize the viscoplastic behavior of a variety of refractory metals we have undertaken a study of the dynamical properties of molybdenum, tantalum, vanadium and tungsten (all body-centered materials), using time resolved velocity interferometry techniques. The detailed results obtained to date for tungsten, vanadium and tantalum are summarized elsewhere[5,6,7]. In this paper, the more recent results on molybdenum are summarized. The experiments were conducted over a pressure range of 6.5 to 15 GPa. Most of the physical phenomena of interest contribute significantly to the observed wave behaviour for loading and unloading in this pressure range. The viscoelastic behavior of molybdenum can be deduced from the rise time (and release time) measurements of stress or particle velocity profiles. Specific viscoelastic properties of interest include the Hugoniot Elastic Limit (HEL), its dependence on run distance and final stress amplitude, the strain rate in the plastic loading wave, properties of release, reshock and release/reshock cycles, and yield strength in the shocked state; metallurgical properties of virgin and recovered material are also of interest. These measurements are the first of this nature for fully dense molybdenum, although preliminary results of this study have been reported elsewhere[9].

The objective of the present paper is to present the data obtained from the experiments conducted with molybdenum and interpretations of the loading/unloading properties.

Impact Experiments

We performed a matrix of ten impact experiments on a 4" single-stage compressed gas gun. Shot geometries are schematically shown in Figure 1, omitting spall rings around the projectile tip and such experiment-specific details as flush pins, velocity pins and turning mirrors. Dimensions and densities of critical components are summarized in Table I. A Velocity Interferometer System for Any Reflector (VISAR)[10] was used to monitor the velocity history of an aluminized, diffusely reflecting interface in the target between the sample and a sapphire window. A Z-cut sapphire window[1,2] was chosen because its high shock impedance in the 0-15 GPa range is well matched with that of molybdenum. In this pressure range the sapphire behaves elastically, which provides the added advantage of simplified interpretation of the data for those experiments utilizing a sapphire impactor.

The molybdenum was tested in an as-received condition. Optical metallography showed the molybdenum microstructure consists of a partially recrystallized equiaxed grain structure with a fine grain size of nominally 3-5 μm.

Velocity histories for all tests are shown in Figure 2. These fall into four categories, according to experiment type. Tests CrMo 1 and 2 provide a loading wave followed by a release wave. Tests CrMo 3, 4, 7, 9, and 10 provide a loading wave, release wave, then a second loading wave. Tests CrMo 5, 6 and 8 provide a loading wave followed by a reshock, then a release. Impact time on all velocity histories was established by assuming a toe velocity matching our measured longitudinal ultrasonic velocity of 6.295 mm/μsec. In the present paper, we have chosen to con-

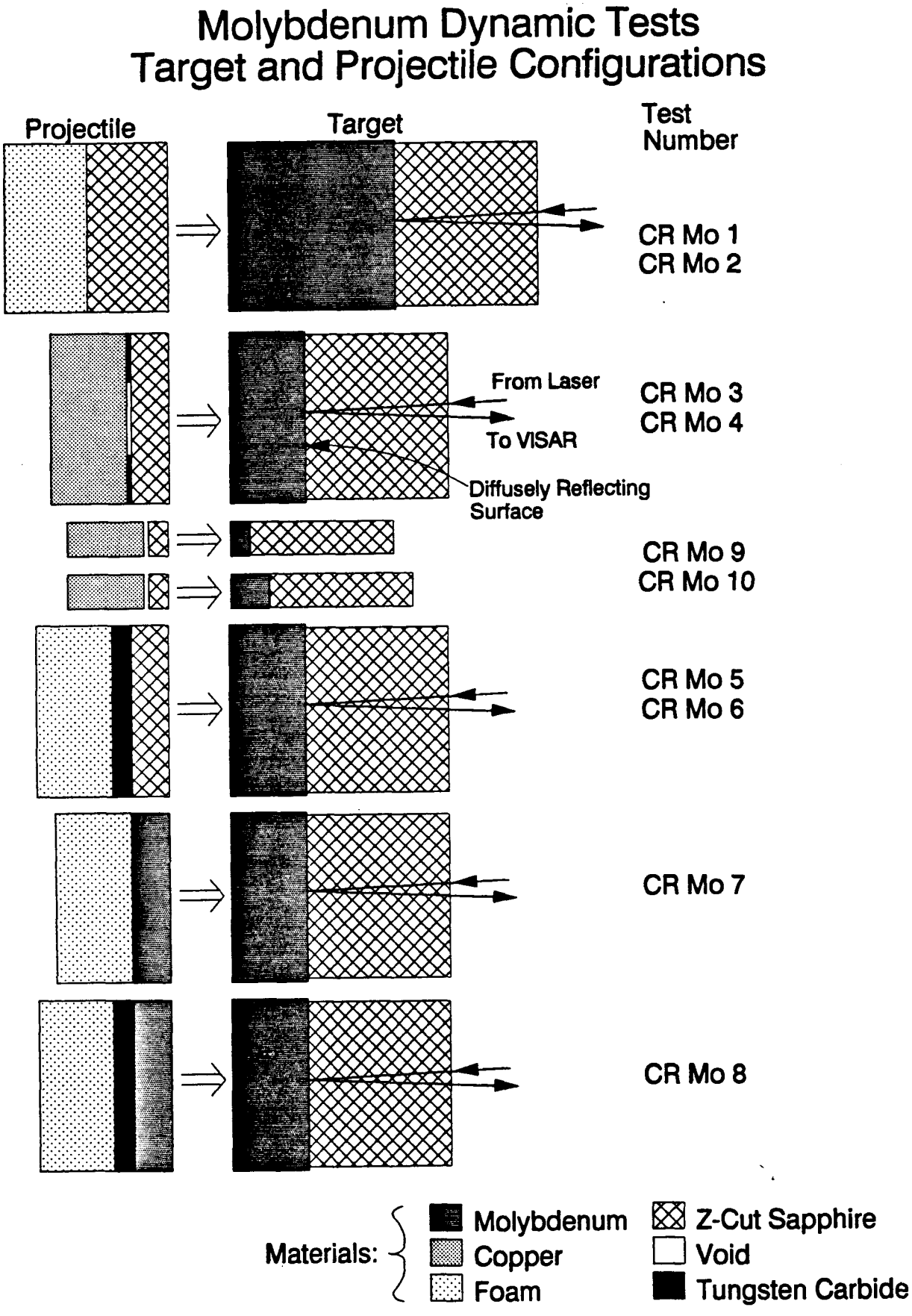

FIGURE 1.
Schematic test geometries for the present experiments. Tests CrMo 9 and CrMo 10 are similar to tests CrMo 3 and CrMo 4, except for different sample and flyer plate thicknesses.

Table I. - Dimensions of Important Components for Molybdenum Tests

Test -->	CrMo1	CrMo2	CrMo3	CrMo4	CrMo5	CrMo6	CrMo7	CrMo8	CrMo9	CrMo10
					Projectile Components					
Foam or Copper[1]:										
Dia.[2]	50.736	50.675	50.775	50.780	50.820	50.820	50.795	50.810	50.825	50.825
Thick	6.7792	6.8531	6.0316	6.031	6.4254	6.4498	6.403	~ 6	3.001	3.021
ρ_0[3]	0.295	0.295	8.920	8.9185	0.295	0.279	0.296	0.293	8.87	8.87
Space or Tungsten Carbide (if present)[4]:										
Dia.	--	--	1"/2"	1"/2"	50.897	50.886	--	50.858	1.375"/2"	1.375"/2"
Thick	--	--	0.297	0.3235	1.594	1.588	--	1.5946	0.200	0.202
ρ_0	--	--	1.16	1.18	14.820	14.880	--	14.904	~1.19	~1.19
Impactor (Sapphire or Molybdenum)[5]:										
Dia.	50.798	50.806	50.838	50.790	50.802	50.820	44.534	44.547	50.810	50.807
Thick	6.3474	6.3408	3.010	3.011	2.997	2.9986	3.000	2.999	1.576	1.5766
ρ_0	3.976	3.980	3.972	3.975	3.973	3.971	10.071	10.200	3.96	3.96
					Target Components					
Molybdenum:										
Dia.	45.194	45.18	53.353	53.373	53.370	53.343	45.197	45.194	53.378	53.365
Thick	13.0566	13.046	6.1620	6.1265	6.118	6.1062	6.1163	6.1183	1.5306	3.023
ρ_0	10.211	10.16	10.204	10.215	10.221	10.2198	10.216	10.2136	10.193	10.200
Sapphire[6]:										
Dia.	50.848	50.843	50.875	50.838	50.941	50.858	50.834	50.950	50.127	50.952
Thick	25.38	25.32	25.252	25.385	25.399	25.390	25.392	25.395	25.033	25.389
ρ_0			3.982	3.98	3.980	3.979	3.981	3.981	3.98	3.98
Impact Vel.	450.18	260.0	256.4	437	250	447.5	522	521.8	278.5	275.7
VPF	40.72	40.358	40.358	40.72	40.358	40.72	40.72	40.72	40.358	40.358

1. Tests 3, 4, 9 and 10 use copper; all others use foam here
2. Diameters and thicknesseses in mm, except for spacer diameters (in inches, as indicated)
3. Densities in grams per cubic cm
4. Tests 3, 4, 9 and 10 have spaces (voids) formed by 2" diameter Lexan spacers (OD 2", ID 1" or 1.375") of the thickness and approximate density indicated.
5. Molybdenum impactors for tests 7 and 8; sapphire impactors for all other tests.
6. Explicit densities not available for tests 1 and 2; presumed similar to other tests.

FIGURE 2.
Velocity histories observed by VISAR at the molybdenum-sapphire interface for the configurations shown in Figure 1.

centrate on the time intervals of the velocity histories shown in Figure 2. These may be interpreted without worry about edge effects contaminating the one-dimensional nature of the experiment.

All of the experiments providing a reshock of the Hugoniot state (CrMo 5, 6 and 8) show a brief drop in velocity immediately before the acceleration of the reshock arrives at the VISAR interface (1.42, 1.39 and 1.74 μsec, respectively). This is caused by an infinitesmal thickness of adhesive (a few microns) between the sapphire impactor and the tungsten carbide reshock plate. When the shock propagating through the sapphire impactor encounters this layer of adhesive, a release will begin propagating back through the impactor and the molybdenum sample. A reshock is produced several nanoseconds after the release, but travels at a lower velocity than does the release. The time separation widens, to give the observed pullback signature. Under these circumstances, the sample experiences a slight release prior to reshock. Such phenomena may have also occurred in older experimental work, but have remained undetected due to poorer time resolution in those studies.

Interpretation of Loading and Load-Release Profiles

All wave profiles were analyzed by an explicit Lagrangian calculation comparing input and output wave profiles for the sample. This analysis yielded tabular relations between wave speed, stress, strain, strain rate, particle velocity and window velocity. For those experiments with a reshock following the initial shock (CrMo 5, 6, and 8), this analysis was cut off after the initial shock arrival at the window.

Wave Speed Measurements

The Hugoniot state is evaluated as shock velocity vs. particle velocity (Figure 3). Shock velocity is evaluated at the inflection point in a plot of wave speed vs. stress for each test. For the low velocity impacts (approx. 260 m/sec), velocities were measured directly from the middle of the plastic loading wave profiles due to difficulties in measuring the inflection point. These (velocity) profiles are detailed in Figure 4. The shock velocity represents a wave velocity for the plastic wave, which differs from the velocity determined from a stress/strain point under the steady-wave assumption because of the strongly 2-wave loading structure.

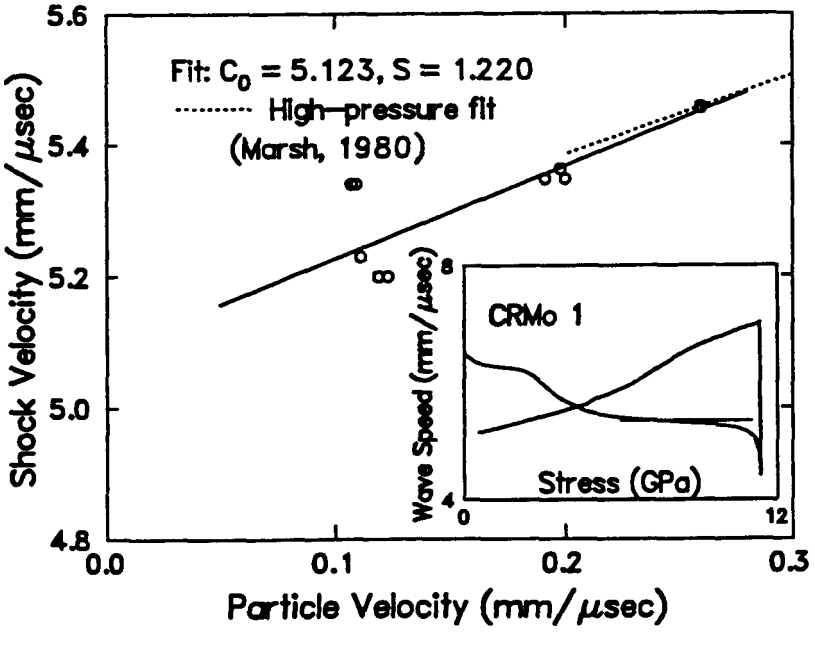

FIGURE 3
Shock velocity - particle velocity Hugoniot measured for fully dense molybdenum. Circles represent points from the present study. Inset depicts how shock velocity is chosen. Dotted line is from data in Marsh[11].

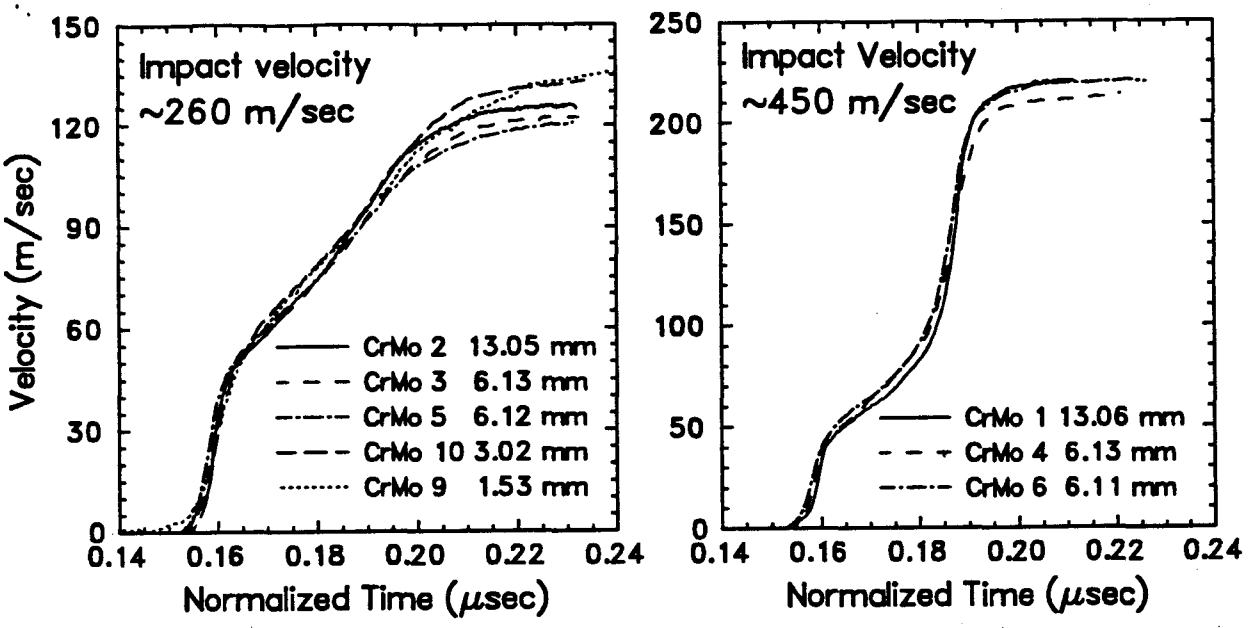

FIGURE 4
Wavefront stacks, normalized for 1 mm thick samples.

Strain rates were calculated by smoothing $\Delta\sigma/\Delta\tau$. For each test, a value representing the overall peak was chosen from a plot of this function (sample curve shown in Figure 5). These values correspond closely to values obtained directly from the shock slope in the velocity history $(dU_p/dt)/U_s$. Large values of strain rate for low stresses represent the elastic wave in the sample shown. This peak value is plotted against the maximum Hugoniot stress in Figure 5. As can be seen, the strain rate varies approximately as the fourth power of the final stress. This is in agreement with the observations for many other metals[12].

The loading waves appear to be steady over the 1.5 - 13 mm range for the 6-7 GPa final stress level and over the 6 -13 mm range for the ~11 GPa level, as illustrated in Figure 4. Similarly, the strain rate systematically decreases with travel distance for these stress levels.

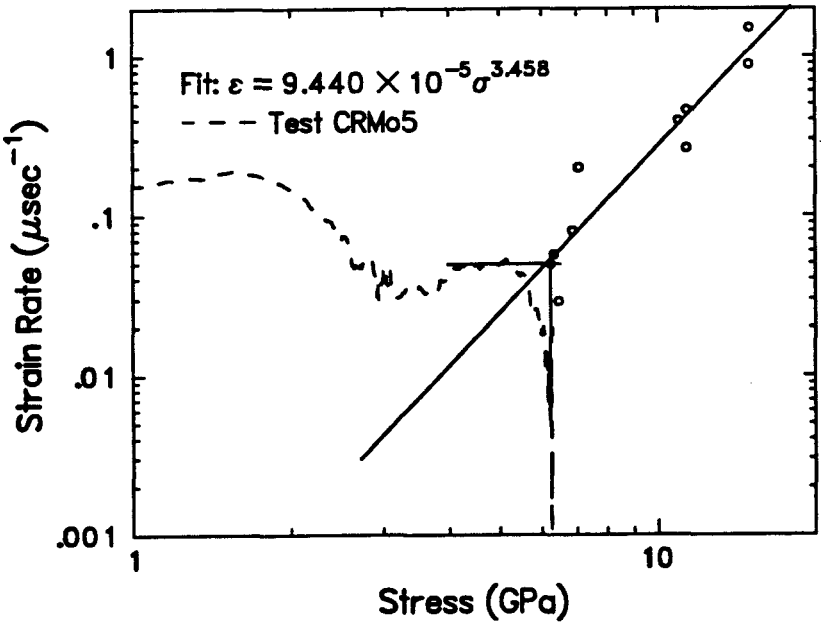

Figure 5.
Stress-strain-rate behavior of molybdenum. Points represent data from the present study. A typical curve from the present study is shown, which is associated with the data point at the intersection of the two line segments.

Hugoniot Elastic Limit Measurements

The HEL was measured from a plot of wavespeed against stress, with a yield strength determined from the relation, $Y = \sigma(1-2\nu)/(1-\nu)$, with ν = Poisson's ratio. The HEL varies from 2.3 to 2.8 GPa, with Y correspondingly varying from 1.3 to 1.6 GPa (ν taken as 0.301). Values for the HEL and uncertainties are estimated in stress-wave-speed space as shown in Figure 6.

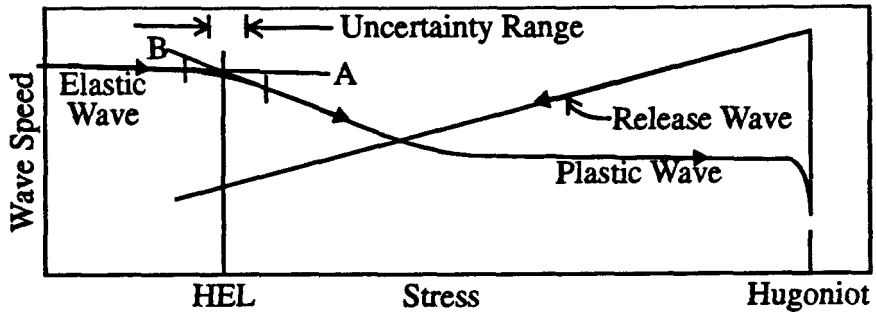

FIGURE 6.
Measurement of HEL. The HEL is taken as the intersection of lines A and B, with uncertainties extending halfway to the point of tangency of these lines with the wave profile.

For the HEL, no dominant trend with propagation distance or peak stress is observed over a propagation distance of 1.5 mm to 13 mm (ie. the sample thicknesses). There appears to be a slight decrease of the HEL with increasing propagation distance.

Yield Strength in the Shocked State

The yield strength of material at the Hugoniot state may be determined as 3/4 of the width of the stress/strain loop. Alternatively, for stress regimes where shock heating is minimal, it may be calculated as 3/2 of the offset between the Hugoniot and the hydrostat (ie. delta stress at constant strain). For fully dense molybdenum, the hydrostat has been determined to 10 GPa by Manghnani and Ming[13] and may be written in terms of the Birch-Murnighan equation with K_0 = 267 GPa and K' = 4.46. This hydrostat is plotted against the results of the present study in Figure 7. The experimental results suggest that the yield strength of the material in the shocked state is comparable to that determined at the HEL; this is demonstrated in Figure 8.

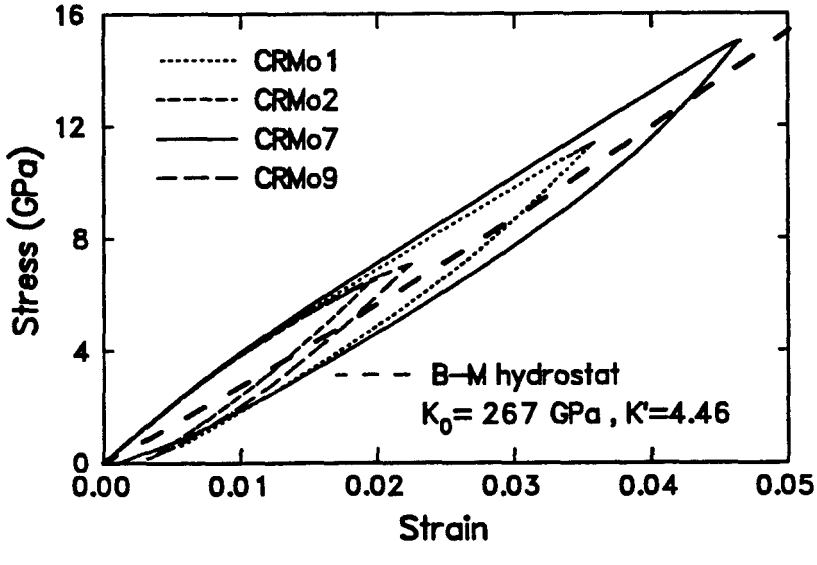

FIGURE 7
Stress-strain trajectories calculated for four representative tests on fully dense molybdenum.

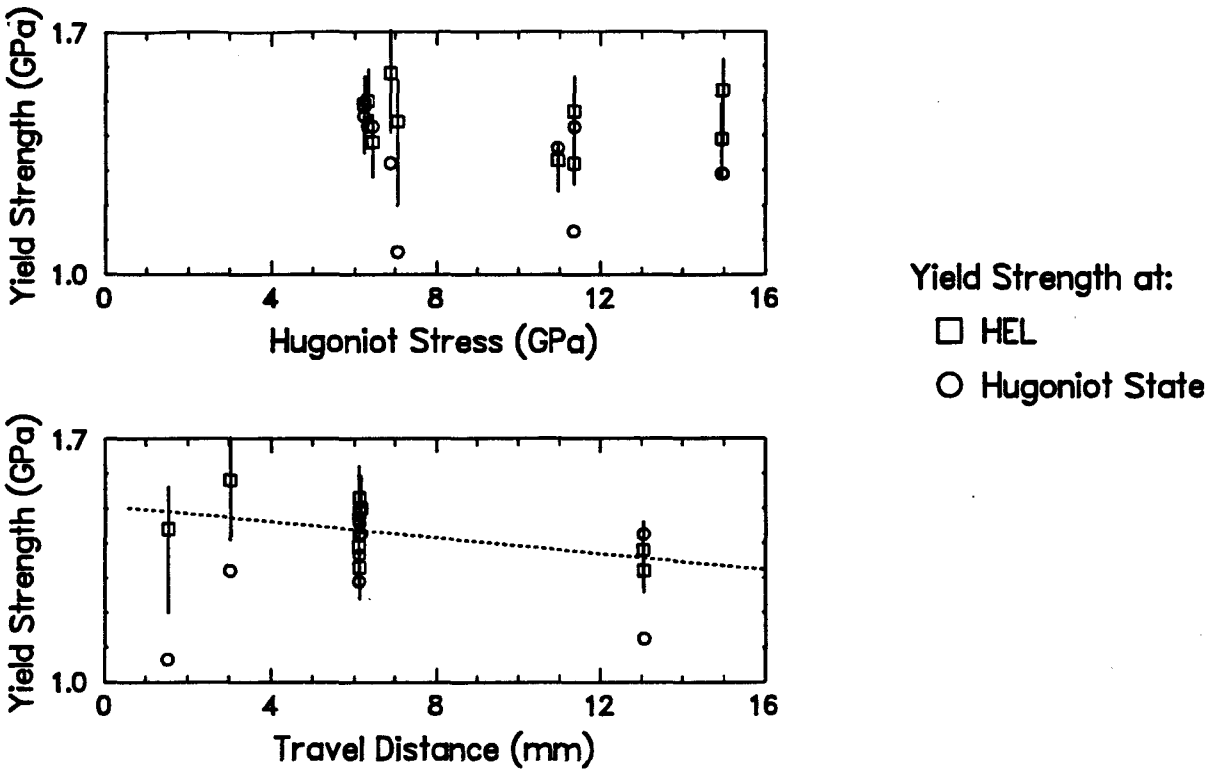

Figure 8.
Yield strength at the Hugoniot state and the HEL, plotted against Hugoniot stress and travel distance. Representative uncertainties in strength at the HEL (method of Fig. 6) are shown. Dashed line is a least-squares fit for strength at the HEL.

Table II presents many of these results in numerical form, including strengths computed using the hydrostat.

Neither procedure for determining strength is entirely satisfactory. As seen in Figure 7, the hydrostat passes slightly below the middle of the stress-strain loops for the lower-pressure representative experiments. Shock heating may play a very minor role; for CRMo 1, the rise of 20°C will cause a decrease in volumetric strain of approximately 0.001 (7°C and 0.0004 for CRMo 2). The more important factor is probably experimental error in determining the absolute positions of the shock and static EOS. On the other hand, choosing a loop width requires measuring from yield surface to yield surface, which is barely possible for low stresses, such as CRMo 2, which are largely a reflection of elastic behavior. A more sensitive technique to determine yield strength in the shocked state as described by Asay and Chhabildas[14] is currently underway.

Lower-strain-rate experiments

For comparison with the gas-gun experiments, Hopkinson bar and strain machine tests have been performed. The true stress-true strain response of molybdenum was measured as a function of strain rate (10^{-3} to $5 \cdot 10^{3}$ sec^{-1}) and temperature (77 to 298 K). The yield strength of molybdenum is seen to increase with strain rate and decrease with increasing temperature. Values for the strength at 298K range from ~750 MPa at a strain rate of 10^{-3} s^{-1} to 1500 MPa at a strain rate of 5000 s^{-1}. At 77K, yield strength values range from 1750 MPa at a strain rate of 10^{-3} s^{-1} to a level of 1935 MPa when loaded at 2000 s^{-1}. This ~2.5 fold increase in yield strength with temperature drop combined with strain rate rise is reasonably typical of the high strain rate and temperature sensitivity of bcc metals (eg. vanadium[8]). This also reflects the high lattice friction (Peierls barrier) in these metals.

Table II. - Selected Shot, HEL and Hugoniot Parameters for Molybdenum Tests

Test -->	CrMo1	CrMo2	CrMo3	CrMo4	CrMo5	CrMo6	CrMo7	CrMo8	CrMo9	CrMo10
HEL (GPa)	2.325	2.43	2.63	2.33	2.61	2.58	2.45	2.69	2.53	2.78
Range[1]:	2.21-2.44	2.26-2.57	2.52-2.80	2.18-2.41	2.37-2.76	2.32-2.75	2.25-261	2.41-2.85	2.11-2.74	2.48-3.01
Y_0 from HEL (GPa)[2]	1.32	1.38	1.50	1.33	1.49	1.47	1.39	1.53	1.44	1.58
Range:	1.26-1.39	1.28-1.46	1.43-1.59	1.24-1.37	1.35-1.57	1.32-1.57	1.28-1.49	1.37-1.62	1.20-1.56	1.41-1.71
Hugoniot Strain	0.0355	0.0195	0.0192	0.0341	0.0189	0.0355	0.0464	0.0464	0.0223	0.0211
Hugoniot Stress (GPa)	11.35	6.45	6.33	10.96	6.24	11.36	14.95	14.97	7.06	6.88
Hugoniot Stress - Hydrostat (GPa)	0.75	0.95	0.95	0.91	0.97	0.95	0.86	0.86	0.71	0.88
Hugoniot Strength (GPa)[3]	1.125	1.425	1.425	1.365	1.455	1.425	1.29	1.29	1.065	1.32
Shock Velocity (mm/μsec)	5.35	5.23	5.34	5.35	5.34	5.36	5.45	5.46	5.20	5.20
Particle Velocity (mm/μsec)	0.200	0.111	0.109	0.191	0.107	0.198	0.260	0.260	0.123	0.119
Strain Rate[4] (μsec^{-1})	0.264	0.029	0.057	0.393	0.049	0.457	0.885	1.506	0.200	0.080

1. Hugoniot Elastic Limit and range measured as depicted in Fig. 7
2. Calculated assuming a Poisson's ratio of 0.301
3. Calculated using deviation from hydrostat
4. From smoothing curve from Lagrangian analysis

Discussion and Conclusions

The primary conclusions which we draw from this study concern material strength and viscoelastic properties for molybdenum under high strain-rate conditions. These are:

- The HEL stress level measured in this study is approximately 2.5 GPa (yield strength of approximately 1.45 GPa), and appears to decrease slightly with propagation distance over the range 1.5 - 13 mm.
- The loading wave is very nearly steady over the propagation distance of 1.5 - 13 mm for shocks of 6 to 11 GPa strength; it is therefore probably steady over this propagation range for stronger shocks.
- The yield strength of the shocked state is ~1.4 GPa, comparable to the yield strength measured from the HEL.
- The fourth-power dependance of strain rate on stress is valid for molybdenum in the parameter space of these experiments.
- The Hugoniot in this pressure range is consistent with the higher-pressure Hugoniot derived from older methods.

The experimentally measured HEL stress level of ~2.5 GPa is in fairly good agreement with calculations by Follansbee[15], which predict a stress level of 2.9 GPa. His model allows the estimation of the HEL from lower strain-rate experiments by assuming that stress-strain behavior is controlled by a thermally activated interaction of dislocations with obstacles both in the HEL and conventional strain rate regimes. Using arguements based on standard thermal activation theory, he predicts that the HEL will lie below the yield stress at 0 K, termed the mechanical threshold stress, for a number of metals. For molybdenum, the above quasi-static and dynamic yield data may be converted to the uniaxial stress-strain state of the shock and used in this theory to give the calculated HEL of 2.9 GPa.

The similarity between the calculated and measured HEL supports the implication that the same thermally activated interaction of dislocations with obstacles controls behavior in the conventional strain rate and HEL regime. Furthermore, the similarity of both of these quantities with the strength of the Hugoniot state suggests that these processes may also be important under the conditions of the Hugoniot state. Further analysis of the reshock experiments may give more information here.

Acknowledgements

The authors gratefully acknowledge guidance and motivation from D. Steinberg. They are also appreciative of helpful discussions with and calculations by P. S. Follansbee, and low strain-rate experiments by G. T. Gray III. Thanks are due as well to Jeff Miller for performing the gun tests. This research was supported by the U.S. DOE under contract #DE-AC04-76DP00789.

References

1. L. C. Chhabildas, Survey of diagnostic tools used in hypervelocity impact studies, Int. J. Impact Engng, 5, 205-220, 1987.

2. L. C. Chhabildas and R. A Graham, Development in measurement technique for shock-loaded solids, in AMD 73, ASME Publishers, NY, 1987.

3. J. R. Asay and G. I. Kerley, The response of materials to dynamic loading, Int. J. Impact Engng, 5, 69, 1986.

4. L. Davison and R. A. Graham, Shock compression of solids, Physics Reports 55, 255, 1979.

5. L. C. Chhabildas and L. M. Barker, Dynamic quasi-isentropic compression of tungsten, pp. 111-114 in Shock Waves in Condensed Matter - 1987, S. C. Schmidt and N. C. Holmes, eds., Elsevier Science Publishers B.V, 1988.

6. L. C. Chhabildas, L. M. Barker, J. R. Asay and T. G. Trucano, Relationship of fragment size to normalized spall strength for materials, Int. J. Impact Engng, 10, 107-124, 1990.

7. L. C. Chhabildas and J. R. Asay, Dynamic yield strength and spall strength measurements under quasi-isentropic loading, to be published in the proceedings of the 1990 Explomet Conference, "Shock Waves and High Strain Rate Phenomena in Metals", edited by L. E. Murr, K. P. Staudhammer and M. A Meyers, 1991.

8. L. C. Chhabildas and C. R. Hills, Dynamic shock studies of vanadium, pp. 429-448 in Metallurgical Applications of Shock-Wave and High-Strain-Rate Phenomena, L. E. Murr, K. P. Staudhammer and M. A. Meyers (eds.), Marcel Dekker, 1986.

9. M. D. Furnish, L. C. Chhabildas, D. J. Steinberg and G. T. Gray III, Dynamic behavior of fully dense molybdenum, in Shock Waves in Condensed Matter - 1991, S. C. Schmidt, R. D. Dick, J. W. Forbes and D. G. Tasker, Elsevier Science Publishers B.V., in press.

10. L. M. Barker and R. E. Hollenbach, Laser interferometer for measuring high velocities of any reflecting surface, J. Appl. Phys, 43, 4669-4675, 1972.

11. S. P. Marsh (ed.), LASL Shock Hugoniot Data, University of California Press, 1980.

12. J. W. Swegle and D. E. Grady, Shock viscosity and the prediction of shock wave rise times, J. Appl. Phys., 58, 692, 1985.

13. L. Ming and M. H. Manghnani, Isothermal compression of bcc transition metals to 100 kbar, J. Appl. Phys., 49, 208-212, 1978.

14. J. R. Asay and L. C. Chhabildas, Determination of the shear strength of shock-compressed 6061-T6 aluminum, p. 417 in Shock Waves and High Strain-Rate Phenomena in Metals, M. A. Meyers and L. E. Murr, eds., Plenum Publishers, 1981.

15. P. S. Follansbee, The HEL and rate-dependent yield behavior, pp. 349-352 in Shock Compression of Condensed Matter - 1989, S. C. Schmidt, J. N. Johnson and L. W. Davison (eds.), Elsevier, 1990.